REVEALING THE HIDDEN STRUCTURE OF COASTAL SEDIMENT TRANSPORT PATHWAYS USING LAGRANGIAN COHERENT STRUCTURES

STUART G. PEARSON[1,2], AD RENIERS[1], & BRAM VAN PROOIJEN[1]

1. *Delft University of Technology, Department of Hydraulic Engineering, Delft, 2600GA, The Netherlands.* s.g.pearson@tudelft.nl, a.j.h.m.reniers@tudelft.nl, b.c.vanprooijen@tudelft.nl
2. *Deltares, Department of Applied Morphodynamics, Delft, 2600MH, The Netherlands.*

Abstract: Understanding coastal sediment transport pathways is essential for effective management of coastal systems. To quantify the patterns underlying these pathways (Lagrangian Coherent Structures), we calculate Finite Time Lyapunov Exponents (FTLE) in the sediment transport velocity field using a sediment transport particle tracking model, SedTRAILS. We simulate an idealized sandy tidal inlet system over the course of a single tidal cycle. Here we show that FTLE patterns indicate barriers to sediment transport and zones of sediment dispersal. These patterns can be used to inform strategic placement of sediment for coastal nourishments and to develop testable hypotheses explaining sediment pathways.

Introduction

Coasts and estuaries evolve under the influence of complex hydrodynamics and morphodynamic feedbacks. Underlying these morphodynamic changes are a series of hidden patterns in the sediment transport pathways. It is essential that we better understand these patterns because of their effect on coastal management concerns like nourishment dispersal, channel infilling, coastal erosion, and ecological impacts of human interventions.

To this end, we developed SedTRAILS (Sediment TRAnsport vIsualization & Lagrangian Simulator), a Lagrangian sediment transport model which tracks the motion of sediment particles at O(10^2-10^4 m) scales (Pearson et al., 2021). In order to reveal the hidden structure underlying the sediment pathways, we identify Lagrangian Coherent Structures (LCS) in the sediment velocity field. LCS are commonly used in coastal and oceanographic applications to describe mixing and frontal systems in hydrodynamic flow fields (Reniers et al., 2010; Kuitenbrouwer et al., 2018). Here we propose a novel analysis of LCS in coastal sand transport fields, where LCS reveal barriers to sediment transport and zones of sediment mixing, accumulation, or dispersal, essential concepts for coastal engineering and management.

Methodology

To demonstrate our method, we consider an idealized sandy tidal inlet. Our approach features 3 main steps (Fig. 1):

(i) Simulate hydrodynamics with D-Flow FM model.
(ii) Estimate Lagrangian sediment pathways using SedTRAILS model.
(iii) Compute Finite-Time Lyapunov Exponent (FTLE) field.

We elaborate on these steps in the following sections.

Fig. 1. Overview of the four main steps to deriving Lagrangian coherent structures (LCS): (i) derive the Eulerian sediment transport fields; (ii) compute Lagrangian sediment pathways; (iii) compute Finite Time Lyapunov Exponents to approximate the Lagrangian Coherent Structures.

Eulerian Hydrodynamic Modelling

First, we use D-Flow FM (Deltares, 2022) to numerically model the depth-averaged (2DH) hydrodynamics of an idealized tidal inlet (3 km long, 1 km wide) and basin (23 x 13 km) (Fig. 2). The model domain measures 60 x 40 km in size, with the finest grid resolution of 150 m in the inlet area. We focus our analysis on an 8 x 9 km region surrounding the inlet. The seabed in the inlet and basin is set at a constant level of -3 m MSL and is considered fixed during the simulation. An M2 tide (with range of 1.8 m) propagates eastward alongshore. In the centre of the inlet, the tide is ebb-dominant with maximum currents of 1.6 m/s. Shore-normal waves of H_s = 3.5 m, T_p = 7 s are introduced at the seaward boundary. A Chezy coefficient of 65 $m^{1/2}/s$ is used to account for bed friction.

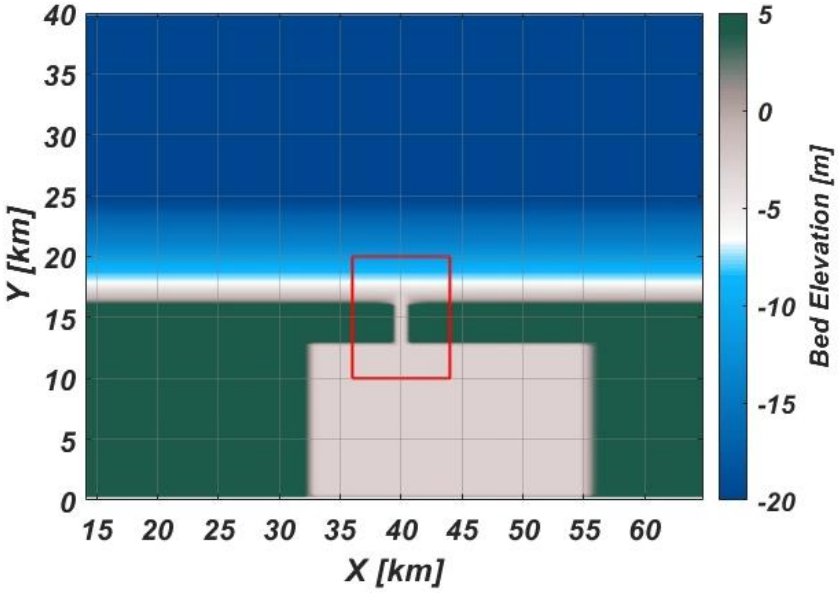

Fig. 2. Overview of D-Flow FM model bathymetry featuring inlet and basin (bed level of -3m). The bed elevation remains static throughout the simulation. Subsequent analyses focus on the area surrounding the inlet, indicated by the red box.

Sediment Particle Tracking Modelling

To estimate sediment transport pathways, we used SedTRAILS, a MATLAB-based offline particle tracking model (Pearson et al., 2021). SedTRAILS generates the sediment transport velocity field u_{gr} (Fig. 3a) for sand-sized particles (d_{50} = 200 µm) using the method of Soulsby et al. (2011):

$$u_{gr} = P \cdot R \cdot U_c \quad (1)$$

where P is a probability of motion between 0 and 1 depending on the exceedance of critical shear stress, R is a velocity reduction factor based on the dominant mode of transport (i.e., particles move faster as suspended load than bed load), and U_c is the flow velocity at a given point. We do not yet consider burial or mixing of particles within the seabed – a "concrete" bed, meaning that particles are always available for remobilization.

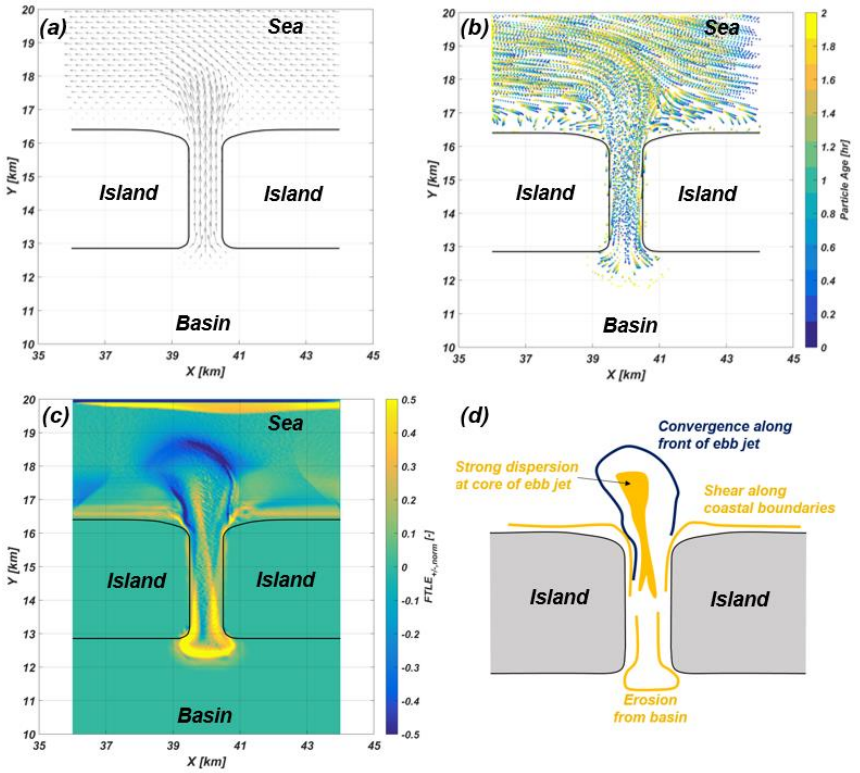

Fig. 3. Overview of the main steps to deriving Lagrangian coherent structures (LCS) in sediment velocity fields at an idealized tidal inlet, shown here at ebb tide. (a) Compute sediment transport vector field; (b) derive sediment particle trajectories; (c) compute Finite Time Lyapunov Exponent (FTLE) field (T = 2 hours); (d) interpret FTLE field as Lagrangian Coherent Structures.

Sediment particles are then advected by this sediment transport velocity field, and their positions are represented by:

$$\frac{d}{dt}\boldsymbol{x}(t) = \boldsymbol{u_{gr}}(\boldsymbol{x}(t), t) \qquad (2)$$

where $\boldsymbol{x}$ represents the position of the particle in space, and $\boldsymbol{u_{gr}}$ is the spatially and temporally-varying sediment transport velocity field. This approach considers purely advective transport without diffusion.

We advect sediment particles forward in time for a 6-hr window every 10 mins over the course of an M_2 tidal cycle. We then repeat the procedure, instead advecting sediment particles backward in time over the same intervals. The resulting pathways then form the basis for subsequent analyses.

Compute Finite Time Lyapunov Exponent (FTLE)

To derive Lagrangian Coherent Structures, we use MATLAB to compute the Finite-Time Lyapunov Exponent (FTLE) from forward and backward particle trajectories as per Haller (2015) and Krishna et al (2021). The flow map Φ for a given period T is computed for each point in a regular grid of 20,000 particles initially spaced at $\Delta x = 200$ m and $\Delta y = 250$ m and released at t_0 (Fig 3b):

$$\boldsymbol{\Phi}_{t_0}^{t_0+T}: \boldsymbol{x}(t_0) \mapsto x(t_0) + \int_{t_0}^{t_0+T} v(x(\tau), \tau)\, d\tau \tag{3}$$

The Jacobian matrix of partial derivatives of the flow map $D\Phi$ quantifies the spreading or convergence of neighbouring pairs of particles over T relative to their initial positions:

$$\left(\mathbf{D}\boldsymbol{\Phi}_{t_0}^{t_0+T}\right)_{i,j} = \begin{bmatrix} \frac{\Delta x_i(t_0+T)}{\Delta x_i(t_0)} & \frac{\Delta x_j(t_0+T)}{\Delta y_j(t_0)} \\ \frac{\Delta y_i(t_0+T)}{\Delta x_i(t_0)} & \frac{\Delta y_j(t_0+T)}{\Delta y_j(t_0)} \end{bmatrix} =$$

$$\begin{bmatrix} \frac{x_{i+1,j}(t_0+T)-x_{i-1,j}(t_0+T)}{x_{i+1,j}(t_0)-x_{i-1,j}(t_0)} & \frac{x_{i,j+1}(t_0+T)-x_{i,j-1}(t_0+T)}{y_{i,j+1}(t_0)-y_{i,j-1}(t_0)} \\ \frac{y_{i+1,j}(t_0+T)-y_{i-1,j}(t_0+T)}{x_{i+1,j}(t_0)-x_{i-1,j}(t_0)} & \frac{y_{i,j+1}(t_0+T)-y_{i,j-1}(t_0+T)}{y_{i,j+1}(t_0)-y_{i,j-1}(t_0)} \end{bmatrix} \tag{4}$$

From this matrix, the Cauchy-Green deformation tensor $\Delta i,j$ is calculated as:

$$\boldsymbol{\Delta}_{i,j} = \left(\mathbf{D}\boldsymbol{\Phi}_{t_0}^{t_0+T}\right) * \left(\mathbf{D}\boldsymbol{\Phi}_{t_0}^{t_0+T}\right) \tag{5}$$

Where * denotes the transpose of the matrix. We can then determine the Finite Time Lyapunov Exponent $\sigma_{i,j}$, which indicates regions with exponentially divergent particle trajectories:

$$\sigma_{i,j} = \frac{1}{|T|} \ln \sqrt{(\lambda_{max})_{i,j}} \tag{6}$$

Where T is the integration time and λ_{max} is the largest eigenvalue of $\Delta i,j$ for each particle i,j. We select an integration time T of 6 hours to capture the dynamics on tidal timescales. Shorter timescales do not result in clearly-defined FTLE ridges, and longer timescales obscure the behaviour occurring at each stage of the tidal cycle.

Ridges of high forward FTLE values correspond to repelling Lagrangian coherent structures in the sediment transport field. Conversely, ridges of high backward FTLE values correspond to attracting Lagrangian coherent structures in the sediment transport field, where sediment shears or converges in forward time. These attracting structures consequently act as barriers to transport. In Figs. 3 & 4, FTLEs are normalized such that forward (repelling) FTLEs are positive (yellow) and backward (attracting) FTLEs are negative (blue) as per d'Ovidio et al. (2004).

Results

Sediment Particle Tracking Modelling

At ebb-tide, particles are advected seaward as a jet, which is then swept westward alongshore by the shore-parallel tides (Fig. 3b). At flood tide (not shown), the ebb jet is deflected eastward and particles are advected into the inlet. These particles accumulate inside the basin, forming a pattern that resembles an incipient flood tidal delta. In both cases, there is limited movement of particles within the basin, since velocities there are not high enough to move 200 μm sand grains at locations more than 1-2 km from the inlet.

Lagrangian Coherent Structures

The spatial patterns of LCS vary with each stage of the tidal cycle (Fig. 4). First, we consider the backward (attracting) FTLEs (blue). At ebb tide (Fig 4a, t=06:30), FTLE-b ridges form along the expanding boundaries of the ebb jet. The most pronounced ridge forms along the eastern edge of the ebb jet, where the alongshore tidal current collides with it and many particles converge. At the beginning of the flood tide (Fig. 4b, t=09:50), the ebb jet is advected eastward with the alongshore tidal current. Inflowing currents at the mouth of the inlet pinch off the base of the ebb jet and FTLE-b ridges form in the channel, akin to tidal intrusion fronts (i.e., Largier, 1992). These ridges are advected towards the basin, where they accumulate just inside its entrance (Fig. 4d, t=14:50). Ridges at the lateral offshore boundaries are associated with edge effects and do not directly correspond to regions of convergence.

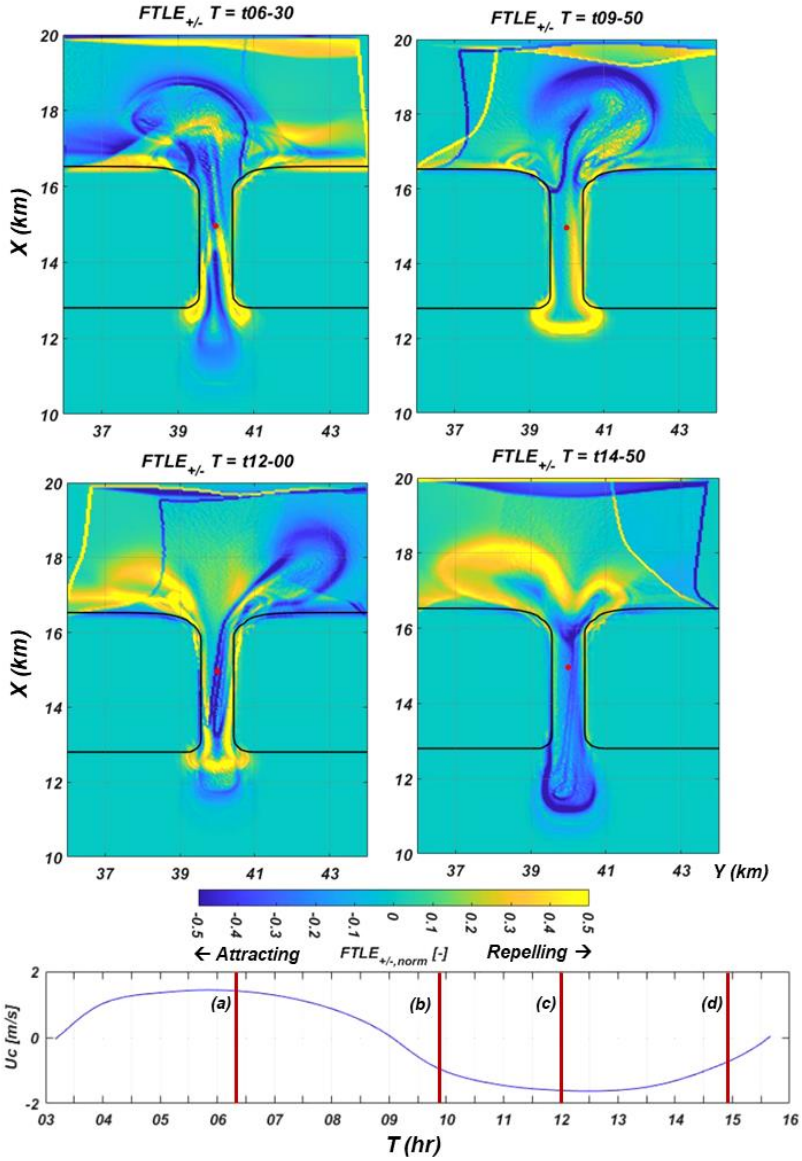

Fig. 4. Snapshots of FTLE field (T = 6 hours) at different stages of the tidal cycle. (a) ebb tide, (b) early flood tide, (c) peak flood tide, (d) high water slack. Positive (yellow) FTLE values indicate highly dispersive zones, while negative (blue) FTLE values indicate highly convergent zones. Velocities are positive to the north, measured at the red dot in the centre of the inlet. Solid black lines indicate the 0 m elevation contour.

We next consider the forward (repelling) FTLEs (yellow). At ebb tide (Fig 4a, t=06:30), there are two high FTLE-f regions flanking the basin's entrance which can be explained by particles there being ejected from the basin and far from their neighbours. As the flood jet within the basin wanes (Fig. 4b, t=09:50), these marginal regions expand to the entire basin entrance. During the flood tide (Fig. 4c,d), analogous FTLE-f lobes develop at the seaward mouth of the inlet, where particles become sucked into the basin and greatly separated from their neighbours. Throughout much of the tidal cycle, FTLE-f ridges are high along the margins of the channel.

Discussion

Interpretation of Lagrangian Coherent Structures

FTLE analysis has been widely used to quantify LCS hidden within coastal and oceanographic flows, and here we present a novel application of this technique to reveal the patterns underlying sand transport at an idealized tidal inlet. Areas of convergence corresponding to backward FTLE ridges are barriers to sediment transport, while areas of divergence corresponding to forward FTLE ridges are highly dispersive. However, high FTLE values may also be explained by zones of intense shear (e.g., at channel walls), which are not truly convergent. Further analysis using the techniques outlined in Haller (2015) can help differentiate these shear zones.

The information obtained using this approach can be used to explain sediment pathways obtained using tracer studies or numerical models (e.g., Pearson et al., 2021). In particular, this method allows us to better understand the patterns underlying sediment transport at tidal timescales. Residual transport patterns averaged over longer periods (months to years) determine morphological changes, but gross transport patterns at these shorter timescales remains under-examined. These patterns are relevant for human interventions in the coastal system, such as the placement of sediment for nourishments.

Next Steps

After demonstrating a proof of concept for this technique in an idealized context, the next steps will be to apply it to real study sites with sufficient data for calibration and validation (e.g., drifter studies, radar data, and sediment tracers). Potential sites include Ameland Inlet in the Netherlands (Elias et al., 2022) and the mouth of the Columbia River in the US (Stevens et al., 2020).

Knowledge of sediment transport patterns and pathways is essential for strategic placement of sediment as part of building with nature or beneficial reuse programs. For example, placing nourishments may require careful timing and positioning to ensure that the sediment reaches the target area efficiently (e.g., Baptist et al., 2019). Sediment could be placed on the opposite side of a transport barrier to avoid deposition in an ecologically sensitive area.

Furthermore, the present analysis opens up new hypotheses to test in future research. Since backward (forward) FTLEs correspond to zones of convergence (divergence), they should indicate depositional (erosional) zones. Persistent FTLEs may thus indicate regions of morphodynamic change. Saddle points between forward and backward FTLEs both attract and then repel particles, so they correspond to energy-efficient trajectories through a flow field (Krishna et al., 2022) and regions of enhanced mixing (d'Ovidio et al., 2004). Persistent saddle points could thus represent nodes on key sediment transport pathways.

Conclusions

Here we present a novel approach to interpreting Lagrangian sediment transport model output via the application of finite-time Lyapunov exponents (FTLE). The Lagrangian coherent structures (LCS) revealed by FTLE analysis at an idealized tidal inlet indicate barriers to sediment transport and zones of sediment mixing, accumulation, or dispersal, which are important concepts for coastal engineering and management. The spatial patterns of LCS vary in space and time with the different stages of the tidal cycle. Areas of convergence corresponding to backward LCS ridges are barriers to transport, while areas of divergence corresponding to forward LCS ridges are highly dispersive. This approach also presents new opportunities for testing hypotheses about the patterns underlying sediment transport pathways.

Acknowledgements

This publication is part of the TRAILS project (with project number 17600) in the research programme ‘Living Labs in the Dutch Delta’, which is (partly) financed by the Dutch Research Council (NWO).

References

Baptist, M. J., Gerkema, T., van Prooijen, B. C., van Maren, D. S., van Regteren, M., Schulz, K., ... & van Puijenbroek, M. E. B. (2019). Beneficial use of dredged sediment to enhance salt marsh development by applying a ‘Mud Motor’. *Ecological Engineering*, 127, 312-323.

Deltares (2022). D-Flow Flexible Mesh: Computational Cores and User Interface User Manual. https://content.oss.deltares.nl/delft3d/manuals/D-Flow_FM_User_Manual.pdf

d'Ovidio, F., Fernández, V., Hernández-García, E., & López, C. (2004). Mixing structures in the Mediterranean Sea from finite-size Lyapunov exponents. *Geophysical Research Letters*, 31(17).

Elias, E. P., Pearson, S. G., van der Spek, A. J., & Pluis, S. (2022). Understanding meso-scale processes at a mixed-energy tidal inlet: Ameland Inlet, the Netherlands–Implications for coastal maintenance. *Ocean & Coastal Management*, 222, 106125.

Haller, G. (2015). Lagrangian coherent structures. *Annu. Rev. Fluid Mech*, 47(1), 137-162.

Kuitenbrouwer, D., Reniers, A., MacMahan, J., & Roth, M. K. (2018). Coastal protection by a small scale river plume against oil spills in the Northern Gulf of Mexico. *Continental Shelf Research*, 163, 1-11.

Largier, J. L. (1992). Tidal intrusion fronts. *Estuaries*, 15(1), 26-39.

Pearson, S.G., Elias, E.P.L., van Ormondt, M., Roelvink, F.E., Lambregts, P.M., Wang, Z.B., & van Prooijen, B. (2021). Lagrangian sediment transport modelling as a tool for investigating coastal connectivity. In Coastal Dynamics Conference 2021.

Reniers, A. J., MacMahan, J. H., Beron-Vera, F. J., & Olascoaga, M. J. (2010). Rip-current pulses tied to Lagrangian coherent structures. *Geophysical Research Letters*, 37(5).

Soulsby, R. L., Mead, C. T., Wild, R., & Wood, M. (2011). A Lagrangian model for simulating the dispersal of sand-sized particles in coastal waters. *Journal of waterway, port, coastal, and ocean engineering*, 137(3).

Stevens, A. W., Elias, E., Pearson, S., Kaminsky, G. M., Ruggiero, P. R., Weiner, H. M., & Gelfenbaum, G. R. (2020). *Observations of coastal change and numerical modeling of sediment-transport pathways at the mouth of the Columbia River and its adjacent littoral cell* (No. 2020-1045). US Geological Survey.